Astron. & Astrophys. 46, 49–59 (1976)

Results on the Cosmic Ray Chemical Composition at Energies up to 100 GeV/nucl.

W. K. H. Schmidt, K. Atallah*, T. F. Cleghorn**, W. V. Jones***, A. Modlinger**** and M. Simon
Max-Planck-Institut für Physik und Astrophysik, Institut für extraterrestrische Physik, Garching

Received May 21, 1975

Summary. Some aspects of the chemical composition of high energy cosmic rays have been investigated in a balloon flight in 1972 from Palestine, Texas. The apparatus used was an ionization spectrometer with a geometric factor of 1.01 m^2sr. The charge resolution was sufficient to separate four groups of elements from the CNO group to the iron group. The energy range covered extends up to 100 GeV/nucl. The results indicate that there is no drastic change in abundance ratios at high energies, and that at 100 GeV/nucl. spallation products are still present. However the high energy abundance ratio between the CNO group and the iron group is about a factor of two different from that one that was reported for low energies of about 1 GeV/nucl. by other authors.

Key words: cosmic rays — chemical abundances

1. Introduction

In this paper we describe measurements of the chemical composition of cosmic rays as a function of energy in the range of a few GeV/nucleon to typically 100 GeV/nucleon. The results were obtained by using a balloon borne, very shallow ionization spectrometer. This spectrometer was very shallow because we wanted to trade off energy resolution for geometric factor. The resulting geometric factor of about 1m^2sr enabled us to determine the chemical composition of cosmic rays up to the quoted energies.

The depth of the ionization spectrometer and the geometric factor were compromised upon within the weight constraints for balloons. The final payload weighed about 2100 kg. The balloon was flown on October 12/13, 1972, from Palestine Texas. It floated for 14 hours at an average residual atmospheric pressure of 6.7 mb. At the end of the flight the parachute failed to deploy properly and then failed catastrophically, so that after a free fall the payload was completely destroyed. Thus it was impossible to repeat the flight as planned with a different absorber configuration; but data of the flight reported were received via telemetry during the total time at float, and the results of the analysis of this flight are reported here.

* Now at Technische Universität, Munich, Germany.
** Now at Lockheed Electronics, Houston, Texas.
*** Permanent address: Dept. of Physics and Astronomy, Louisiana State University, Baton Rouge, Louisiana.
**** Now with Entwicklungsring Nord, Bremen, Germany.

2. Experimental Details

A detailed description of the instrument has been given elswhere (Atallah *et al.*, 1974). Here a short description will suffice. The apparatus consisted basically of three parts: (1) A scintillation and a Cerenkov counter for charge determination of the incident particle. (2) Spark chambers for trajectory determination. (3) An ionization spectrometer for energy determination. A schematic cross section drawing of the apparatus is shown in Fig. 1. This shows at the same time the dimensions of the apparatus. The sensitive area was 1m × 1m, and the depth between top and bottom scintillators was about 65 cm, yielding a geometric factor of 1.01 m^2sr. The egg-shaped line in Fig. 1 indicates the shape of the pressure vessel that the apparatus was situated in for balloon flights. The pressure was kept to about one atmosphere throughout the flight.

The scintillation counter and Cerenkov counter were built for maximum uniformity of light collection efficiency as a function of position of particle traversion.

The spark chamber consisted of 5 gaps of wire chambers with magnetostrictive readout. Unfortunately, it did not work very well, particularly for the higher charges (sparks were missing for higher charges), and therefore no spark chamber information was used in the data presented here (exept that the spark chamber was used for calibrating and mapping with the aid of singly charged particles). As will be shown in the next section we were still able to resolve charge

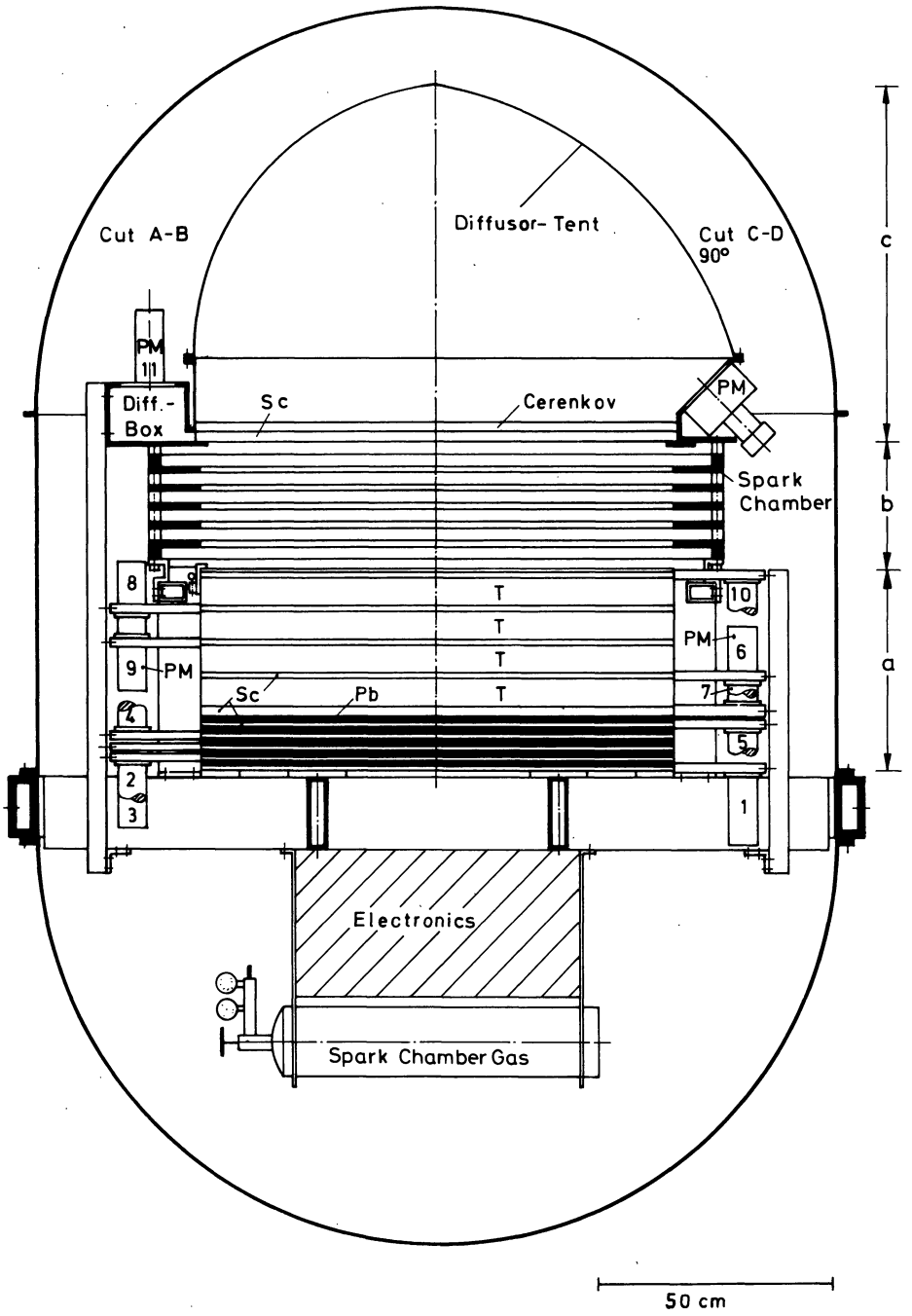

Fig. 1a–c. Schematic cross section drawing of the apparatus consisting of an ionization spectrometer (a), spark chamber (b), and a scintillation and plastic Cerenkov counter for charge determination (c)

groups and therefore get some results on the energy dependence of the charge composition.

Immediately below the spark chamber there was the ionization spectrometer. It consisted of a total of about 12 radiation lengths (rad.l.) of lead interleaved with plastic scintillators. The spaces marked *T* on Fig. 1 contained only a quarter of a rad.l. of lead each. It was intended to fill these "target" spaces by a quarter of a rad.l. of graphite, each, for the second balloon flight. As mentioned before, the second flight did not take place due to the destruction of the apparatus after the first flight. The target was made exchangeable because we intended to separate protons and electrons on a statistical basis: High energy electron cascades behave exactly alike in the quoted amount of lead or carbon (Atallah *et al.*, 1974). However, for protons the lead target consisted of only 0.03 interaction lengths (int.l.) while the graphite target consisted

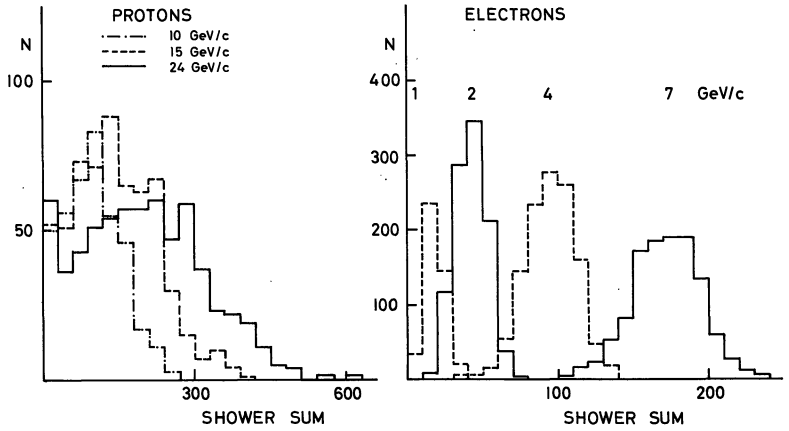

Fig. 2. Shower sum distributions from both exposures to high energy electrons and protons. In case of protons, only events that interacted in the target were used

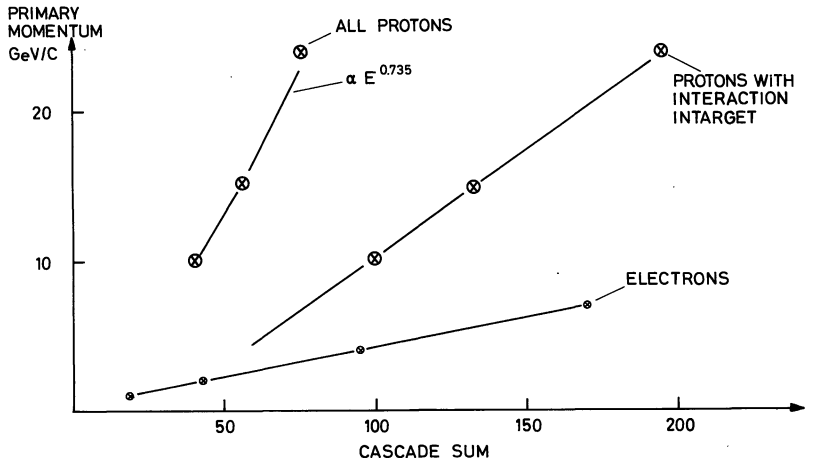

Fig. 3. Averages of proton and electron induced showers as functions of primary momentum

of 0.5 int.l. of matter. Assuming then that cosmic ray intensities do not change between balloon flights, it would have been possible to determine the electron and proton intensities by comparing event rates of both flights with different targets.

For calibration, a small version of the absorber stack was used. A 30 cm × 30 cm functional model of the absorber section only, that is without charge module and spark chamber, was exposed to 10, 15 and 24 GeV/c protons at CERN, and to 1, 2, 4 and 7 GeV/c electrons at DESY. Figure 2 shows signal distributions, and Fig. 3 shows the energy dependence of the average signals (see also Atallah *et al.*, 1974).

3. Charge Determination

The Cerenkov counter was made from Pilot Plastic 425 (containing a wave length shifter) of dimension 1 m × 1 m × 3/4″. The light was collected from a light diffusion box which was roughly dome shaped. It was painted white on the inside with a paint which was basically $BaSO_4$. The scintillator was made from Pilot B plastic scintillator of the same size as the Cerenkov counter, but the light was taken from two opposite edges of the scintillator. The scintillation light was guided into two lengthy light diffusion boxes and was there collected by two phototubes each.

As has been mentioned already the scintillation counter and Cerenkov counter were built for maximum uniformity of light collection efficiency. This way it was possible to separate charge groups despite the failure of the spark chamber for high charges. The uniformity of these detectors was determined by observing the average pulse height for muon traversal for sections 10 cm × 10 cm wide. The average signals of these 100 cells form a distribution of

signals, and the standard deviation of this distribution divided by the overall average signal, was $\sigma \approx 10\%$ for the scintillation counter and $\sigma \approx 5\%$ for the Cerenkov counter.

For vertically incident sea level muons we collected an average of 4.2 photoelectrons on the combined photocathodes of 4 tubes of 5″ diameter (RCA 4525) from the Cerenkov counter, and about 40 photoelectrons on the combined photocathodes of 4 tubes of 2″ diameter (VALVO XP 1001) from the scintillator. The four photoelectrons from the Cerenkov counter ensure a separation of four standard deviations between signals from adjacent charges of relativistic particles. This separation is constant over the full range of charges by virtue of the Z^2 dependence of the Cerenkov signal, so that adequate charge separation was ensured if zenith angle dependence of the signal could be compensated for. Except for zenith angle dependence the Pilot 425 material is possibly scintillating, and the scintillation could be a possible cause of deviation from Z^2 proportionality of the signal, as it is found in plastic scintillators. We checked the Pilot 425 for scintillation light (Atallah and Schmidt, 1974) and found that less than 5% of the total light yield from relativistic particles was scintillation light (upper limit) so that we are reasonably sure that saturation effects of the signal play only a negligible role.

The signal distribution for one particular element at the rather high cutoff of Palestine/Texas is washed out by positional nonuniformity of light collection, zenith angle dependence according to the $\sec\theta$—pathlength distribution, and any additional zenith angle dependence of the Cerenkov light (due to its directionality). The path length distribution for the particular geometry employed is shown in Fig. 4. This was calculated and verified experimentally within statistical errors. The full width at half maximum is about 10% of the left edge. The average angle of incidence on our apparatus was about 27°. The zenith

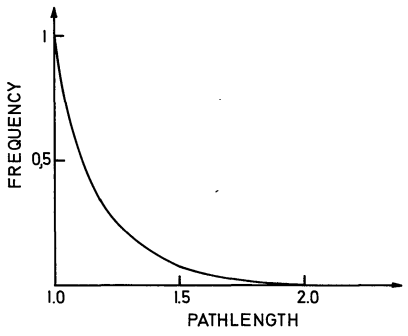

Fig. 4. Calculated path length distribution for particles traversing the apparatus, with telescope requirement between top and bottom scintillators. The ordinate shows the relative frequency of a particular path length, the abscissa shows the path length in units of thickness of the detector under consideration

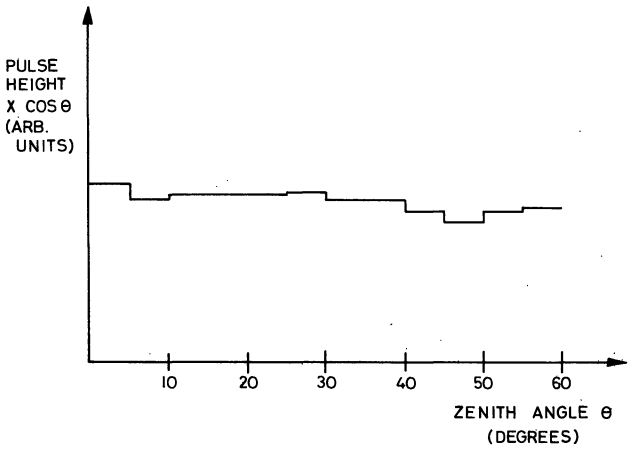

Fig. 5. Zenith angle dependence of the Cerenkov counter signal. The ordinate shows output signal per unit path length, the abscissa shows the angle between the particle trajectory and the figure axis of the apparatus (zenith angle)

angle dependence of the Cerenkov counter signal, normalized per unit path length (of the particle inside the plastic material) is shown in Fig. 5. Since this is almost constant over the possible angles of incidence it does not contribute significantly to the charge resolution.

Figure 6 shows a scatter plot of the Cerenkov counter signal versus the top scintillator signal. The coordinates show the square root of the signal, which was first expressed in "minimum ionizing particle" units and calibrated with sea level muons on the ground, and penetrating particles of charge one during the balloon flight. The saturation of the scintillator signal is apparent, but the Cerenkov signal shows approximately the charges of the incident particles, and one can see clearly the C−O (M) group, the step to the Ne−Si (LH) group, the valley between S and Fe (MH-group), and the iron group.

Figure 7 shows a histogram of the Cerenkov counter signals of all events between the solid lines of Fig. 6. Again, one can clearly distinguish the mentioned charge groups, and in the case of C and O one can almost separate the two elements, although there is no way to separate the nitrogen. This is due to the fact that the actual signals are proportional to the squares of the charges, and the width of the path length distribution is still small as compared to the separation between the carbon and oxygen signals.

The relative abundances of the various charge groups in Fig. 7 seem to be inconsistent with the usual picture. However Fig. 7 shows data as taken during part of the flight above a certain energy (i.e. triggering) threshold. The ionization spectrometer responds to energy per particle, which is the atomic weight A multiplied by the energy per nucleon. Therefore the

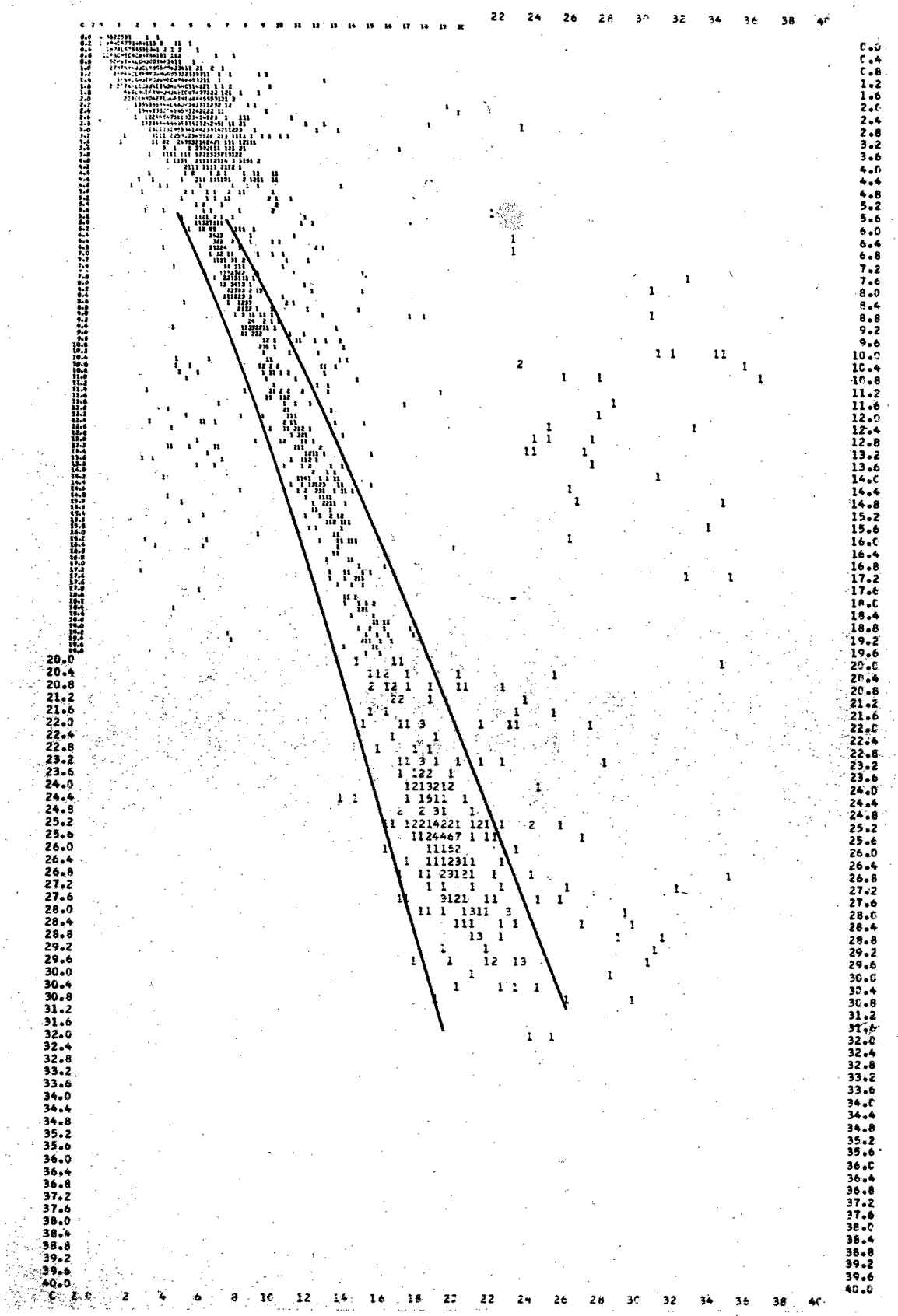

Fig. 6. Scatter plot of the square root of the Cerenkov counter signal (ordinate) *vs* the square root of the top scintillator signal (abscissa). The Cerenkov signal shows approximately units of charges of the penetrating particles. All events between the solid lines were used in the data analysis

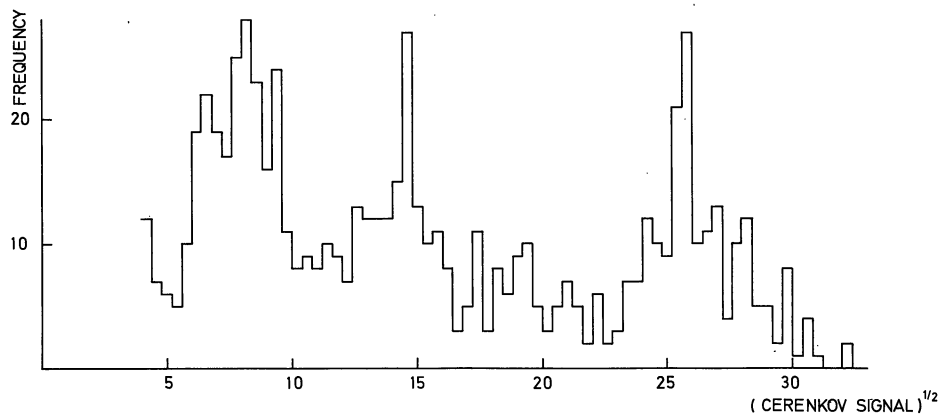

Fig. 7. Charge histogram obtained during part of the balloon flight above a particular energy threshold. The threshold is used for triggering above a certain energy per particle. In terms of energy per nucleon the threshold changes from about 70 GeV/nucl. for Carbon to about 10 GeV/nucl. for the VH group

actual threshold in terms of energy per nucleon varies in Fig. 7 from left to right in such a way that it corresponds to about 70 GeV/nucl. for carbon, and about 10 GeV/nucl. for the iron group.

4. Energy Determination

Figure 2 shows clearly that there is no way of distinguishing between various energies of individual protons events, and even for heavier particles where several nucleons interact in the shallow spectrometer, the fluctuation distributions might remain rather wide. If the fluctuation distribution is known approximately, and it is known not to change too rapidly with energy, then it is still possible to determine energy spectra as long as they are reasonably smooth.

Particularly simple is the case for power law energy spectra. Let $N(E)dE$ be a primary energy spectrum, that is for example the spectrum of a species of cosmic ray nuclei at the place of the measuring device. We call the signal spectrum at the output of the device the "secondary spectrum". S is the measured signal which is suitably normalized so that $\langle S\rangle = E$ for monochromatic input. Let E and S relate in such a way that events of the primary spectrum from the interval between E and $E+dE$ are distributed in S according to the normalized distribution function $f(E,S)dS$. Then the shape of the secondary spectrum is

$$N^+(S)dS = \int_{E=0}^{E\to\infty} N(E)\cdot f(E,S)dSdE\,. \tag{1}$$

If $f(E,S)$ is separable into an energy dependent factor and a factor that is independent of energy E in that sense that it is solely a function of

$$y = \frac{S}{E}, \tag{2}$$

and is normalized so that

$$\int_{y=0}^{y\to\infty} g(y)dy = 1\,, \quad \text{with} \quad f(E,S) = \frac{g(y)}{E}, \tag{3}$$

and if the primary spectrum is a power law of the kind

$$N(E)dE = kE^{-\gamma}dE, \tag{4}$$

then (1) can be rewritten into

$$N^+(S)dS = dS\cdot kS^{-\gamma}\int_{y=0}^{y\to\infty} y^{(\gamma-1)}g(y)dy\,. \tag{5}$$

Hence the secondary spectrum is again a power law spectrum with the same exponent as the primary spectrum. Since for cosmic ray spectra usually $\gamma>1$, one can see that the part of the signal distribution which contains the large signals plays the dominent role. For ionization spectrometers the signal distribution towards large S is limited to a value where S corresponds to 100% of the incident energy so that the integration needs not be carried out to infinity because only finite energies $E>0$ are considered.

In a more general case where $\langle S\rangle$ does not reflect the true primary energy but rather depends on the true primary energy in a nonlinear way, we assume that this functional dependence is given by

$$\langle S\rangle = a\cdot E^{\beta}\,. \tag{6}$$

In that case, instead of (5) we obtain

$$N^+(S)dS = \frac{a}{\beta}^{\frac{\gamma-1}{\beta}} kS^{-\left(\frac{\gamma-1}{\beta}+1\right)}dS\int_{y=0}^{y} y^{\frac{\gamma-1}{\beta}}g(y)dy\,. \tag{7}$$

This is again a power law, but with the exponent of the integral spectrum modified by the factor $1/\beta$.

In order to be able to find the primary spectrum in this simple way we need to know whether (3), (4) and (6) hold approximately. If the primary spectrum is not

a pure power law but has a kink or bend, then this structure will be washed out but still be present in the secondary spectrum. Thus there remains the necessity to check on (3) and (6).

The signal distributions for protons of 10, 15 and 24 GeV/c can be seen in Fig. 2. If normalized they can be shown to conform to requirement (3). However for the very high energies we want to measure, an extrapolation is needed. The only way to extrapolate is by means of Monte Carlo calculations.

Calculations show that there is only little change in the width of the fluctuation distribution towards high energy. One can visualize the reason in the following way: Those events which contribute significantly to the integral on the right of (5) most likely suffer their interaction near the top of the instrument. For late interactions only a small fraction of the energy of the first interaction is dissipated in the apparatus, and therefore y is expected to be small. However for interactions near the top the $\pi^\circ-$ mesons will have 10 to 12 radiation lengths of lead to penetrate. This amount of matter contains the maximum of an electron photon cascade (as is generated by the $\pi^\circ \rightarrow 2\gamma$ decay) up to energies of around 10^3 GeV, and therefore the spectrometer measures essentially the energy contained in the π°-mesons of the first interaction. Therefore the fluctuation distribution reflects to first approximation the inelasticity distribution, and to some extent the number distribution of interactions of the primary particle and the secondary charged π-mesons. Since the inelasticity and cross sections are practically independent of energy over a rather wide range of energies, we expect the measured signal distribution also to be rather constant with energy.

Heavy particles consist of many nucleons, and several nucleons interact on average in a nucleus-nucleus interaction. This should lead to narrower fluctuation distributions. In fact if accelerator events are grouped into groups of 12 events, each of these groups treated as a single event (that is simulating a carbon nucleus composed of 12 independent nucleons at 24 GeV/nucl.) we get a fluctuation distribution with a standard deviation σ divided by the mean μ of $\sigma/u \approx 40\%$. However, the fragmentation probabilities of real nuclei tend to widen the fluctuation distributions again. Monte Carlo calculations yield distributions of width $\sigma/\mu \approx 50\%$ with little change with energy or charge.

The MC calculations were performed with a computer program described earlier (Jones, 1971) and which is continually being tested as new results from accelerator experiments become available.

In order to test Eq. (6) and find the constants a and β we have to rely almost exclusively on Monte Carlo calculations and data from other instruments because the energy range covered at CERN is too small to yield a reliable value of β. From these calculations we find a value for β between 0.72 and 0.75 for protons, and also we find that a power law of the form of (6) fits the calculated results for protons and heavy nuclei well. For heavy nuclei we find values for β only very little less than for protons, so we assume $\beta = 0.735$ for carbon and oxygen, varying to $\beta = 0.720$ for iron group nuclei.

To test the fact that the β-values are practically the same for all nuclei, we note the result (Wdowczyk, 1974) from emulsion measurements by the cosmic ray group of Lodz/Poland that the nuclear cascade builds up as fast as, or may be even faster than a superposition of as many proton cascades as the nucleus contains nucleons. Since the value for β is a measure of the ever increasing "loss of energy out of the bottom of the spectrometer", and this loss depends on the shape of the cascade development, we expect therefore the same value for β for all nuclei. Since the spread in our β values is small we left it as derived from our calculations and like stated above. We note, though, that a larger β for the iron group nuclei would result in a little steeper energy spectrum than reported in Section 5. The value of "a" was found by calibrating Eq. (6) at the geomagnetic cutoff. For all cosmic ray nuclei from Oxygen to iron the geomagnetic cutoff of Palestine/Texas was found to be above the lowest trigger threshold. Calibration of Eq. (6) resulted in a constant "a" that is approximately the same for all nuclei and within 10% of the value derived by the Monte Carlo results. Also, the width of the fluctuation distribution could be tested at energies near the cutoff, and the result of $\sigma/\mu \approx 50\%$ agrees with the MC results.

At this point we have shown how the data on the primary cosmic rays can be derived and to what extent the constants involved can be relied upon. We now proceed to present the data of the balloon flight of October 12/13, 1972.

5. Results

We have shown in Section 4 that charge separation of relativistic particles was possible to a certain extent. In what follows we will use the following nomenclature for the different charge groups: Medium weight nuclei M: $6 \leqq Z \leqq 9$; Leight-heavy nuclei LH: $10 \leqq Z \leqq 16$; Medium-heavy nuclei MH: $17 \leqq Z \leqq 23$; Very-heavy nuclei VH: $Z > 23$. We separate the groups LH and MH between $Z = 16$ and $Z = 17$ because (a) sulfur seems to be present at the sources according to several investigators (Webber *et al.*, 1972; Shapiro *et al.*, 1973a) and (b) due to our insufficient elemental resolution, which smears out the signal distribution towards high values, the place for sulfur might still be dominated by silicon events anyway. We therefore think that by taking MH: $17 \leqq Z \leqq 23$ we have

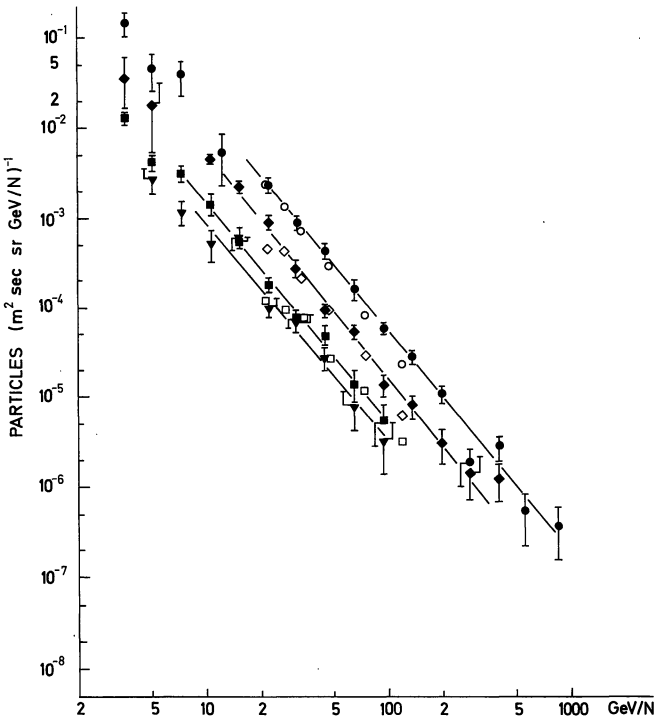

Fig. 8. Energy spectra at the top of the atmosphere of the various groups of nuclei as measured in this experiment (solid symbols), together with the Chicago group's data (Juliusson, 1974) for reference (open symbols). The error bars show statistical errors only. Collective errors in flux might be larger than statistical errors. Error bars of the reference data were omitted to avoid confusion. The symbols stand for M-group nuclei: ● ○; LH-group nuclei: ◆ ◇; MH-group nuclei: ▼; VH-group nuclei: ■ □

selected a fairly clean sample of secondary nuclei, i.e. nuclei that have been mainly created by spallation in interstellar space.

Figure 8 shows spectra at the top of the atmosphere of the various charge groups as defined above. Corrections for interactions in the apparatus, and atmospheric corrections have been applied using the interaction lengths and absorption lengths as reported by Webber *et al.*, (1972). The errors shown are statistical errors only. We realize that there might be errors in flux as well as in slope which are systematic and which are not included in the error bars. Both types of error should be "collective" in the sense that they are roughly the same relatively for all spectra shown. That statement pertains to the atmospheric and overlying matter corrections as well as the correction for the nonlinear energy calibration as expressed in Eq. (6).

The solid lines show maximum likelihood fits to the data. The maximum likelihood fits were made on the assumption that the spectra are pure power law spectra. The χ^2 test shows generally agreement with this hypothesis. The worst χ^2 value found is that for the MH group above 3 GeV/nucl. which is 13.5 for 8 degrees of freedom. The table lists the spectral indeces found. Because of the possible collective errors we do not quote fluxes. We do not quote data points in the immediate vicinity of the geomagnetic cutoff. Equations (1)–(7) hold only in the "equilibrium" part of the spectrum far away from boundaries where the spectrum changes slope or breaks off. Near the lower edge of the spectrum it will be distorted by the fluctuation function. The boundary region will be typically as wide as the fluctuation distribution between mean and upper end. Nuclei deposit on average about 30% of their energy in the spectrometer at energies near the geomagnetic cutoff. That means that there is about a factor of three between the mean and the upper end of the fluctuation distribution. Therefore we are free from boundary effects above the energies quoted. To include lower energies one would have to have very detailed knowledge about the shape of the cutoff and the shape of the fluctuation function, which we are lacking.

An additional correction has been employed in plotting Fig. 8. Using Eqs. (6) and (7) together with the flight parameters the fluxes of the various charge groups can be determined. However it is quite clear that the individual data points do not necessarily represent the actual number of primary events that fall into the respective energy bins. With wide fluctuation functions $g(y)$ with a possible significant tail towards high y-values one rather suspects that the major contribution to a particular data point stems from events of somewhat lower primary energy, because the fluxes are rapidly decreasing with energy.

In order to investigate this in detail we developed a little Monte Carlo computer program, in which we put in a primary power law spectrum of selectable exponent, convolve it with a Gaussian distribution function of selectable width and cutoffs, and then make a maximum likelihood fit to find out the spread in experimental values for the exponent. One result is that the spread in experimental exponents is found to be generally somewhat smaller than the error as returned by a single maximum likelihood fit. This is, as expected, independent of the width of the distribution function used (including zero width, i.e. a delta function). The other result is illustrated in Fig. 9. For a particular "energy interval" of the secondary spectrum we collected the number of events of original or "true" primary energy events into a histogram. Two such histograms are shown in Fig. 9. The distribution functions which are taken to be representative of $g(y)$ are shown as inserts. From all we know it is a fair approximation to take Gaussian density functions for the fluctuation distribution functions, and, after having accepted that fact Fig. 9 shows two things: (a) The width and relative situation of the distribution of original energies is

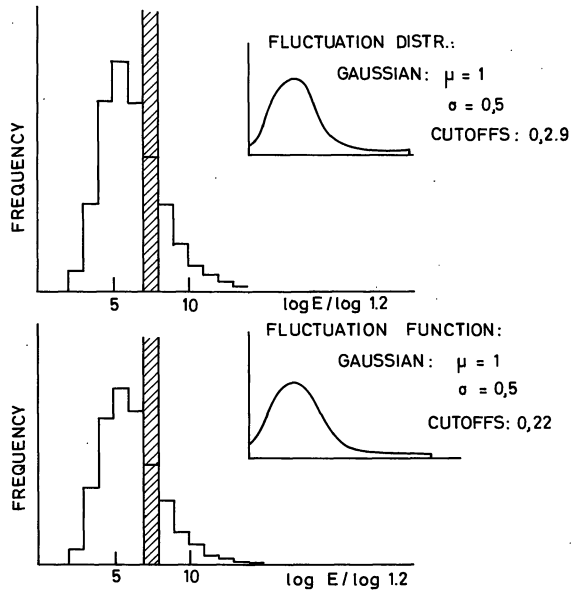

Fig. 9. Results of Monte Carlo calculations of the convolution of a power law distribution (representative of a cosmic ray energy spectrum) with a truncated Gaussian distribution [representative of a wide apparatus fluctuation distribution $g(y)$, see text]. The spectral exponents of the input power laws are indicated, and the Gaussian fluctuation distributions are shown in the inserts. The histograms show the distribution of original events contributing to the hatched bin

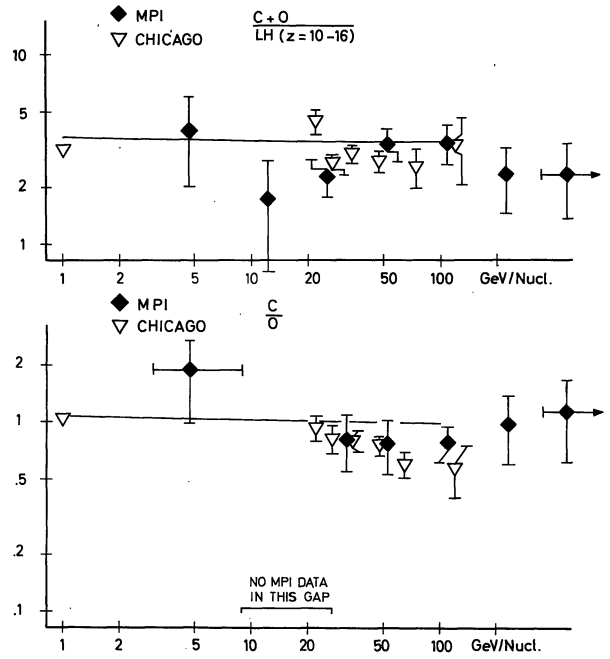

Fig. 10. Ratios of several mainly primary or source elements in cosmic rays. The ratios do not show a significant change with energy. The solid lines are results of model calculations as explained in the text. The Chicago group's data are from Julisson (1974)

rather independent of the length of the tail of the distribution, i.e. the gaussian distribution decreases much more rapidly than the power law primary spectrum of exponent 2.5; (b) The largest contribution to a particular "energy interval" of the secondary spectrum comes from an energy which is about 0.7 of the nominal energy under consideration (of the secondary spectrum), and the distribution of original energies is about a factor of two wide. Therefore we have shifted the data points by a factor of 0.7 in order that they represent better the average energy that contributed to the respective bins.

Since there might be collective errors contained in the spectra as shown in the Table 1 and Fig. 8, it is more informative to consider ratios of different elements in the cosmic rays. In that case, collective errors in the flux cancel, and collective errors in the energy calibration [i.e. an error in β in Eq. (6)] would shift the energy scale only slightly. Figures 10 and 11 show such ratios. Again the data points have been shifted

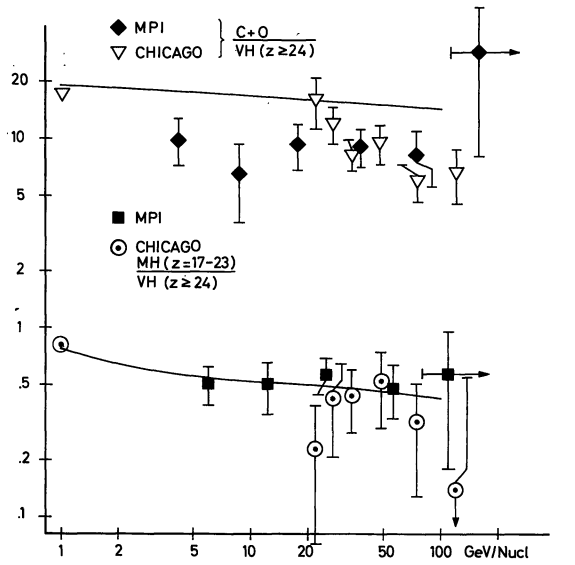

Fig. 11. The top part shows a primary/primary ratio of cosmic ray abundances, and the bottom part a secondary/primary ratio. The solid lines are from the same model calculations as in Fig. 10. The Chicago group's data are again from Juliusson (1974)

Table 1. Spectral indeces (under assumption of pure power laws)

Element group	(Charge range)	γ	Above energy (GeV/nucl.)	γ	Above energy (GeV/nucl.)	Up to energy (GeV/nucl.)
M	(6 – 9)	$2.43^{+0.05}_{-0.06}$	4.3	$2.48^{+0.06}_{-0.07}$	18.6	1000
LH	(10–16)	2.52 ± 0.06	4.3	2.53 ± 0.06	9	500
MH	(17–23)	2.24 ± 0.09	4.3	$2.40^{+0.18}_{-0.17}$	9	115
VH	($\geqq 24$)	2.29 ± 0.08	4.3	2.44 ± 0.15	9	115

by 0.7 in energy; and observe that the data points are about a factor of 2 apart, consistent with the width of the distribution of original energies.

Figure 10 and the top part of Fig. 11 show ratios of elements or groups of elements which are considered to be mostly surviving source elements. The ratio C/O of Fig. 10 has been corrected for the contribution of nitrogen. Since there is no way of separating nitrogen from carbon and oxygen, the separation line was drawn between the nominal places of nitrogen and oxygen. This results in keeping almost all the carbon in the (C+N)-bin and allowing some spill-over of N into the O-bin. After that, a constant fraction of 18% was substracted from the measured C abundance, and 6% was substracted from the measured O abundance. A total of 24% contribution from N is consistent with the integral values above 850 MeV/nucl. from Webber *et al.* (1972). There should be little or no spillover from the O-bin into the (C+N)-bin because due to Landau fluctuations as well as due to the path length distribution of Fig. 4 the charge distribution of an individual charge is skewed towards higher charge values, while having a fairly steep edge towards lower charge values. Thus we note about the ratio as plotted, that since N is mostly a spallation product, its abundance possibly decreases with increasing energy, which has the effect that the plotted C/O ratio would, if anything, have to be raised by a few per cent at very high energies.

Figure 11 shows two groups of data points which are really quite different, apart from their different quantitative values: The ratio M/VH is basically a ratio of abundances of two groups of primary, or source elements. The ratio MH/VH is basically a ratio of abundances between spallation products in interstellar space, and source elements. In all plots data from the Chicago group's results (Juliusson, 1974) have been included for reference. The values shown have been computed from Table 5 of Juliusson (1974).

In all plots of Figs. 10 and 11 solid lines have been drawn. These are from model calculations of cosmic ray propagation which have been carried out under the following assumption: (a) The chemical source composition of cosmic rays is as reported in Shapiro *et al.* (1973b). (b) The path length distribution of cosmic rays at any energy is exponential, for example as in Shapiro *et al.* (1970); (c) Nuclear spallation cross sections were taken from Silberberg and Tsao (1973); (d) The average path length of cosmic rays in the interstellar medium changes with energy in such a way that the L/M ratio fits, within the constraints (a) and (b), the data published in Ramaty *et al.* (1973) as shown in *their* Fig. 2. The functional behaviour of the average path length has been chosen to be a near power law $\lambda^{-1}(\mathrm{g/cm^2})^{-1} = 0.2(E/\mathrm{GeV})^{0.2} - 0.0224$. This model does not necessarily contain the correct interstellar physical conditions. We also realize that there are valid objections to its extension to infinitely high energies. However it does yield the elemental abundance ratios as observed at low energies, and it also fits the *L/M* ratio of Ramaty *et al.* (1973) as function of energy. The calculations were performed in order to see whether such a simple model can explain the behaviour of the heavier elements as a function of energy.

6. Discussion

We have described experimental results and also noted the limitations of their significance. The most serious sources of errors are collective, i.e. the errors should be relatively the same for all particle species considered. Therefore we have plotted ratios of abundances of different particle species in Figs. 10 and 11, and the systematic errors in these ratios should not be more than 10 to 20%.

We feel that we can draw the following conclusions from the data presented in Figs. 10 and 11:

(1) The two sets of data in Fig. 10, and the top part of Fig. 11 show ratios of groups of elements which are considered to be mostly surviving source elements. All three ratios are consistent with constant values as the energy changes. Particularly the C/O ratio extends to very high energies and does not show a severe change in value. The (C+O)/VH ratio is about a factor of two lower than as reported at low energies. Also, several authors have reported a change in this ratio between about 1 GeV/nuc. and several tens of GeV/nuc. (Juliusson, 1974; Ramaty *et al.*, 1973; Ormes *et al.*, 1973; Smith *et al.*, 1973). Unfortunately our data suffer from poor statistics in the low range so that we cannot confirm quantitatively these results. We cannot quite confirm the extremely small (C+O)/VH value of Ormes *et al.* (1973), either. However, at the energies shown our ratio is lower than the low energy ratio, and it does not change any more significantly with energy between several and 100 GeV/nucl.

(2) The only group of elements which are believed to be mainly spallation products from interstellar space and which we were able to separate is the group we call MH. This group in our case contains elements with atomic numbers between 17 and 23. The elements contained in the VH group are the natural progenitors of the MH group. Therefore the ratio MH/VH has been plotted. When we compare the interaction length of the MH group in air with the attenuation length in air as reported in Webber *et al.* (1972), then we reach the conclusion that at least 80% of the MH particles detected were in this group already at the top of the atmosphere. Our conclusion therefore is that spallation products are present up to 100 GeV/nucl. at finite abundances, and therefore we assume that at 100 GeV/nucl. there is still a finite amount of matter that is traversed by cosmic rays between source and observation. This amount is about 2.0 g/cm^2 if the path-length distribution is exponential.

(3) in the energy range covered by this experiment no significant change in the value of the MH/VH abundance ratio can be observed. However, the very low energy data of other authors (Juliusson, 1974; Ormes *et al.*, 1974; Smith *et al.*, 1973; Webber *et al.*, 1974) are somewhat higher. Considering all these data, it appears plausible that there is a change with energy in the abundance ratio between spallation products and their progenitors. And our results favor the conclusion that above several GeV/nucl. this ratio becomes constant with energy, though at a smaller quantitative value than at low energies. However, one group (Smith *et al.*, 1973) has reported results which, although with large errors, do not show a significant change of this energy. It would be desirable to have more data in this energy range in order to clarify this point. The present trend of the majority of the data show clearly a drop in the quantitative value of the abundance ratio with increasing energy, and above 10 GeV/nucl. or so the data shown in Fig. 11 are consistent with no further change or only a very slow further change with energy.

(4) We have taken a simple model of cosmic ray propagation and computed the relative abundances of the element groups as shown in Figs. 10 and 11. The model has been briefly described at the end of Section 5. From Figs. 10 and 11 we conclude that the model is able to describe the data except for the (C+O)/VH ratio. The ratio found experimentally is too low. This can be interpreted as a larger abundance of iron group elements at high energies as compared to low energies. This has been noted before (Ramaty *et al.*) and has been interpreted as a change in source abundances with energy. Under this hypothesis our results seem to indicate that relative source abundances become constant again above several to 10 GeV/nucleon, and at the same time the amount of matter traversed by cosmic rays also becomes energy independent again as indicated by the MH/VH results.

An alternate interpretation seems to be possible: Noting that the ratios (C+O)/VH and MH/VH show qualitatively the same behaviour, with a change with energy below say 10 GeV/nucl., and no change any more above, we wonder whether both ratios couldn't be explained by one effect, namely energy dependent propagation alone. We adopted a "nested leaky box" model of the type first described by Cowsik and Wilson (1973) with an energy dependent leakage lifetime of the particles in the inner box and an energy independent lifetime in the galaxy. This had the effect that – after it was calibrated in the same manner as the simple model for the L/M ratio – we needed more VH nuclei at the sources than in the simple model. Since at high energies, near 100 GeV/nucl., bot models are practically identical, one can see that this would lower the (C+O)/VH ratio. Computations are still in progress, and we cannot quote a best set of parameters for this model, yet. But we feel that a set of parameters can be found, which describes all presently available data well, and therefore we added this note here. This model therefore would describe the changing abundances as seen in cosmic rays on the basis of propagational effects alone, but requires a source composition with a larger iron group content than described in Shapiro *et al.* (1973a).

Acknowledgements. We are pleased to acknowledge the help of the group from Karlsruhe at CERN and of the group from Bonn at DESY. Also we thank H. Arbinger, M. ElHadjAli, E. Hönig and G. Pfaller for their excellent work in designing and constructing this Apparatus.

References

Atallah, K., Cleghorn, T. F., Modlinger, A., Schmidt, W. K. H. 1974, *Nucl. Instr. Meth.* **124**, 461
Atallah, K., Schmidt, W. K. H. 1974, *Nucl. Instr. Meth.* **120**, 539
Cowsik, R., Wilson, L. W. 1973, Conference Papers, 13th Int. CR Conf., University of Denver, Vol. 1, p. 500
Jones, W. V. 1971, Conference Papers, 12th Int. Conf. CR, University of Tasmania, Hobart, Vol. 4, p. 190
Juliusson, E. 1974, *Astrophys. J.* **191**, 331
Ormes, J. F., Balasubrahmanyan, V. K., Arens, J. F. 1973, Conference Papers, 13th Int. Conf. CR, University of Denver, Vol. 1, p. 157
Ramaty, R., Balasubrahmanyan, V. K., Ormes, J. F. 1973, *Science* **180**, 731
Shapiro, M. M., Silberberg, R., Tsao, H. C. 1970, *Acta Phys. Hung* **29**, Suppl. **1**, 471
Shapiro, M. M., Silberberg, R., Tsao, C. H. 1973a, Conference Papers, 13th Int. Conf. CR, University of Denver, Vol. 1, p. 578
Shapiro, M. M., Silberberg, R., Tsao, H. C. 1973b, Conference Papers, 13th Int. Conf. CR, University of Denver, Vol. 1, 578
Silberberg, R., Tsao, C. H. 1973, Naval Res. Lab. Report 7593
Smith, L. H., Buffington, A., Smoot, G. F., Alvarez, L. W., Walig, M. 1973, *Astrophys. J.* **180**, 987
Wdowczyk, J. 1974 (private communication)
Webber, W. R., Damle, S. V., Kish, J. 1972, *Astrophys. Space Sci.* **15**, 245

W. K. H. Schmidt
M. Simon
Max-Planck-Institut für Physik und Astrophysik
Institut für extraterrestrische Physik
D-8046 Garching
Federal Republic of Germany

K. Atallah
Lehrstuhl für organische Chemie und Biochemie
Technische Universität München
D-8000 München 2, Arcisstraße 21
Federal Republic of Germany

T. F. Cleghorn
Lockheed Electronics
16811 Elcamino Real
Houston, Texas 77058, USA

W. V. Jones
Department of Physics and Astronomy
Louisiana State University
Baton Rouge, Louisiana 70803, USA

A. Modlinger
ERNO Raumfahrttechnik GmbH
D-2800 Bremen 1, Hühnefeldstraße 1–5
Federal Republic of Germany